

Detection of coronary plaques using MR coronary vessel wall imaging: validation of findings with intravascular ultrasound

Suzanne Gerretsen · Alfons G. Kessels · Patty J. Nelemans · Jouke Dijkstra ·
Johan H. C. Reiber · Rob J. van der Geest · Marcus Katoh · Johannes Waltenberger ·
Jos M. A. van Engelshoven · Rene M. Botnar · M. Eline Kooi · Tim Leiner

Received: 6 December 2011 / Revised: 29 May 2012 / Accepted: 12 June 2012 / Published online: 11 July 2012
© European Society of Radiology 2012

Abstract

Objectives Compared with X-ray coronary angiography (CAG), magnetic resonance imaging of the coronary vessel wall (MR-CVW) may provide more information about plaque burden and coronary remodelling. We compared MR-CVW with intravascular ultrasound (IVUS), the standard of reference for coronary vessel wall imaging, with regard to plaque detection and wall thickness measurements.

Methods In this study 17 patients with chest pain, who had been referred for CAG, were included. Patients underwent IVUS and MR-CVW imaging of the right coronary artery (RCA). Subsequently, the coronary vessel wall was analysed for the presence and location of coronary plaques.

Results Fifty-two matching RCA regions of interest were available for comparison. There was good agreement between IVUS and MR-CVW for qualitative assessment of presence of disease, with a sensitivity of 94% and specificity of 76%. Wall thickness measurements demonstrated a significant difference between mean wall thickness on IVUS and MR-CVW (0.48 vs 1.24 mm, $P < 0.001$), but great heterogeneity between wall thickness measurements, resulting in a low correlation between IVUS and MR-CVW.

Conclusions MR-CVW has high sensitivity for the detection of coronary vessel wall thickening in the RCA compared with IVUS. However, the use of MRI for accurate

S. Gerretsen · J. M. A. van Engelshoven · M. E. Kooi ·
T. Leiner (✉)
Department of Radiology, Maastricht University Medical Centre,
P. Debyelaan 25,
6229HX Maastricht, The Netherlands
e-mail: t.leiner@umcutrecht.nl

S. Gerretsen · J. M. A. van Engelshoven · M. E. Kooi · T. Leiner
Cardiovascular Research Institute Maastricht (CARIM),
Maastricht University,
Maastricht, The Netherlands

A. G. Kessels
Department of Clinical Epidemiology and Medical Technical
Assessment, Maastricht University Medical Centre,
Maastricht, The Netherlands

P. J. Nelemans
Department of Epidemiology, Maastricht University,
Maastricht, The Netherlands

J. Dijkstra · J. H. C. Reiber · R. J. van der Geest
Department of Radiology, Division of image processing (LKEB),
Leiden University Medical Centre,
Leiden, The Netherlands

M. Katoh
Department of Diagnostic and Interventional Radiology,
HELIOS Clinic,
Krefeld, Germany

J. Waltenberger
Department of Cardiology and Angiology, University of Münster,
Münster, Germany

R. M. Botnar
Imaging Sciences Division, King's College,
London, UK

Present Address:
T. Leiner
Department of Radiology, Utrecht University Medical Centre,
Heidelberglaan 100,
3584CX Utrecht, The Netherlands

absolute wall thickness measurements is not supported when a longitudinal acquisition orientation is used.

Key Points

- Both MRI and IVUS can assess coronary vessels
- Both MRI and IVUS can identify coronary vessel wall thickening.
- MRI provides more information about the coronary plaque burden than conventional angiography.
- However, MRI overestimates absolute coronary wall thickness when compared with IVUS.

Keywords MRI · IVUS · Coronary arteries · Atherosclerosis · Vessel wall imaging

Abbreviations

AUC	Area under the curve
BSSFP	Balanced steady state free precession
CAD	Coronary artery disease
CAG	X-ray coronary angiography
CMRA	Coronary MR angiography
CT	Computed tomography
DIR	Double inversion recovery
FFR	Fractional flow reserve
FWHM	Full width at half maximum
IVUS	Intravascular ultrasound
MESA	Multi-Ethnic Study of Atherosclerosis
MRI	Magnetic resonance imaging
MR-CVW	Magnetic resonance coronary vessel wall imaging
NPV	Negative predictive value
PCI	Percutaneous coronary intervention
PPV	Positive predictive value
PROCAM	Prospective Cardiovascular Münster Heart Study
RCA	Right coronary artery
ROC	Receiver operating characteristic curve
ROI	Region of interest
SPIR	Spectral presaturation with inversion recovery

Introduction

Detection of atherosclerotic plaque can be helpful in individual risk assessment, prevention and treatment of complications of atherosclerosis. For imaging of coronary artery disease (CAD), the current standard of reference is invasive X-ray coronary angiography (CAG). This technique is able to image the coronary arteries with high spatial resolution but is limited to assessment of the coronary lumen. The vessel wall is not visualised with CAG and plaque burden is often underestimated since positive or outward remodelling precedes the development of angiographically detectable stenosis [1, 2].

Positive remodelling refers to a focal compensatory increase in vessel size, due to expansion of the internal elastic lamina, without narrowing of the lumen in response to increasing plaque burden [1, 3, 4]. A study by Schoenhagen et al. [3] found that positive remodelling and larger plaque areas are associated with unstable clinical presentation, showing that complications of atherosclerotic plaques can arise in vessels without a haemodynamically significant stenosis. These findings suggest a potential role for imaging of the coronary vessel wall as a novel tool to improve risk stratification by non-invasive identification of coronary plaques.

The currently accepted standard of reference for in vivo visualisation of coronary vessel wall abnormalities is intravascular ultrasonography (IVUS). At present, IVUS is the most accurate and widely used imaging modality for the assessment of coronary vessel wall geometry in patients, but it is an invasive and costly technique that is not suitable for screening asymptomatic subjects.

Because of its non-invasiveness and the ability to visualise and distinguish soft tissues, magnetic resonance imaging (MRI) has emerged as a potential alternative to IVUS for imaging of the arterial vessel wall [5, 6]. Due to its lack of ionizing radiation, MRI is well suited for serial imaging, offering the possibility to monitor the effect of pharmacological intervention on plaques [7, 8]. Previous studies have demonstrated the capability of MRI to visualise the coronary vessel wall with high spatial resolution as well as vessel wall thickening and positive remodelling in patients [9, 10]. Despite these encouraging results, it remains unclear if and to what extent changes found with MR coronary vessel wall imaging (MR-CVW) accurately reflect true underlying coronary wall thickening.

The aim of this study was to investigate the ability of MR-CVW to accurately detect right coronary artery (RCA) wall thickening and positive remodelling in comparison with the established standard of reference, IVUS.

Materials and methods

Ethics statement

This study was approved by the institutional review board of Maastricht University Medical Centre in Maastricht, The Netherlands. Written informed consent was obtained from all patients prior to inclusion.

Subjects

Consecutive patients with chronic symptoms of chest pain who were referred for CAG or for percutaneous coronary intervention (PCI) or fractional flow reserve (FFR) measurements of already known stenoses were included in this study if they were older than 18 years and after giving written informed consent.

Exclusion criteria were haemodynamic instability, severe arrhythmia and contra-indications for MRI.

MRI protocol

All MRI examinations were performed on a clinical 1.5-T system (Intera, Release 11.1 Philips Medical Systems, Best, The Netherlands) using a dedicated five-element phased-array cardiac coil. Subjects were examined in the supine position. First, localising sequences were obtained and the subject-specific trigger delay and acquisition window were determined. Then, a coronary MR angiography (CMRA) of the RCA was obtained. A three-point plan tool was used to determine the appropriate volume of interest including the entire RCA, resulting in targeted, longitudinal visualisation of the entire RCA in a double oblique plane. For CMRA, we used a bright blood balanced steady state free precession (bSSFP) sequence (TR/TE/FA, 6.2/3.1/120°; in-plane spatial resolution, 0.98×0.98; slice thickness, 3 mm). In the same orientation, a coronary vessel wall sequence was acquired with a proton density weighted 3D fast gradient echo sequence employing radial k-space sampling. A localised double inversion recovery (DIR) prepulse, as previously published [10, 11], was used to visualise the coronary wall. In brief, imaging parameters for the vessel wall sequence were: data acquisition, every other heartbeat; TR, 8.0 ms; TE, 2.0 ms; flip angle, 30°; field of view, 300×300mm; matrix, 384×384. The resulting acquired in-plane spatial resolution was 0.78×0.78 mm with a slice thickness of 3 mm which was reconstructed to 1.5 mm. Subsequently, slices were interpolated to 1.5 mm. Spectral presaturation with inversion recovery (SPIR) was used for fat suppression. For reduction of cardiac motion artefacts, cardiac triggering was used and images were acquired in mid-diastole. To prevent respiratory motion artefacts during this free-breathing acquisition, navigator gating was used to select end-expiratory data. Drift correction was applied during MR data acquisition to prevent decreased navigator efficiency due to diaphragmatic drift during long data acquisition times. The duration of the vessel wall MR sequence was approximately 8.9 min excluding navigator efficiency at a heart rate of 65 beats per second. Total time of the whole MRI session was on average 43.5 min (range 32–71 min) including all preparation sequences, etc.

IVUS imaging protocol

IVUS was not clinically indicated but only used as a research tool. After performing CAG of the RCA, IVUS imaging was performed in the same vessel after administration of 0.2 mg intracoronary nitroglycerine. A commercially available IVUS imaging console (Galaxy 2; Boston Scientific, California, USA) and a 40-MHz catheter (Atlantis SR Pro; Boston Scientific; axial resolution of ± 80 µm, lateral resolution of ± 200 µm)

were used. Images were acquired during continuous pullback at a speed of 0.5 mm/s with 30 frames per second, resulting in a frame thickness of 0.02 mm. No percent stenosis cut-off was set a priori to perform IVUS, since also “normal” segments of the RCA needed to be included for comparison.

Image analysis

For analysis purposes, the RCA was divided into three segments according to the American Heart Association classification [12]. Only the proximal and middle segments of the RCA (segments 1 and 2) were analysed. Due to tortuosity of the coronary arteries and performing measurements on source images instead of multiplanar reformats (MPRs) to prevent reconstruction errors, only short regions of interest (ROIs) could be delineated. Maximum ROI length depended on the visibility in a single slice. Per segment, one ROI in the anterior vessel wall and one ROI in the posterior vessel wall (Fig. 1) were defined in consensus by two observers, who were blinded to IVUS results. This resulted in four ROIs per patient. Areas of the vessel wall were visually graded as thickened as well as non-thickened, and both were included to ensure a mix of diseased and non-diseased ROIs. After selection of ROIs in the MR-CVW datasets, one observer independently matched the MR images with the IVUS datasets using dedicated viewing and analysis software for the IVUS {QCU-CMS (Leiden University Medical Centre, Department of Radiology, Division of Image Processing, Leiden, The Netherlands, in cooperation with MEDIS [13])} and MR datasets (VesselMASS, Leiden University Medical Centre, Department of Radiology, Division of Image Processing, Leiden, The Netherlands [14]), which allow for rotational display of stretched vessel wall views of both the IVUS and MR-CVW images of the RCA. Due to the anisotropic resolution of MR-CVW, reconstructed axial MR-CVW images are not suited for analysis and therefore a stretched view of the IVUS data was reconstructed and compared with the longitudinal MR-CVW data for matching purposes. Selection of the best corresponding IVUS reformat was done by comparing 36 radials through the IVUS data set with the longitudinal MR image: matching was performed by identification of landmarks such as the ostium of the RCA and side branches, and by visual comparison of regions with and without wall thickening. After the best corresponding radial of the reconstructed IVUS image was chosen, the distance of the ROI to landmarks like the ostium of the RCA and the nearest bifurcation points was measured on both MRI and IVUS to be sure that the same region of the vessel was included for measurements.

Each ROI in the MR images was analysed by two observers in consensus regarding the presence of disease. Because of anticipated differences between absolute vessel wall thickness and measured wall thickness due to limitations in spatial resolution of MR-CVW, ROIs were *visually* compared with the rest

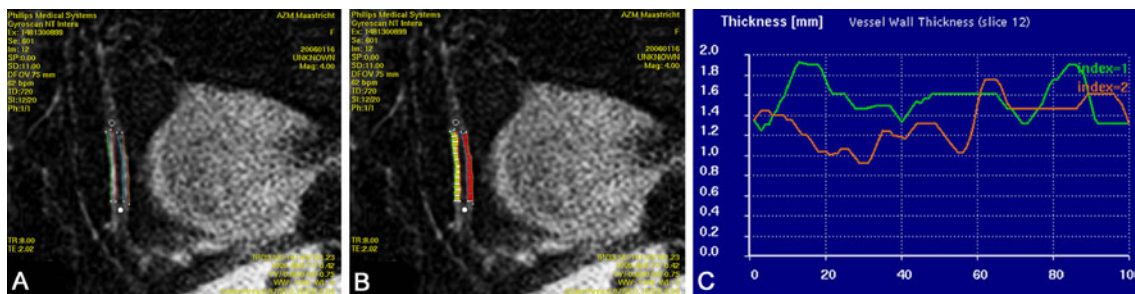


Fig. 1 Measurement of vessel wall thickness on source images. The anterior and posterior vessel walls are delineated as separate ROIs in segment 2 of the right coronary artery (**a**). In each ROI, 100 measurements are made of the anterior (*yellow*) and posterior (*red*) wall thickness

(**b**). The custom-made software program calculates wall thickness over the entire length of the measured ROIs for the anterior (*index 1*) and posterior (*index 2*) vessel wall (**c**)

of the vessel wall. An ROI was considered “diseased” if there was focal vessel wall thickening or clearly increased signal intensity as well as corresponding luminal narrowing compared with adjacent, regularly delineated segments. If there was no luminal narrowing but the vessel wall was thickened compared with the adjacent vessel wall, the ROI was classified as “positive remodelling” and therefore also classified as a diseased segment. ROIs with normal lumen diameter compared with the rest of the vessel and with a vessel wall that had no areas of focal wall thickening or focal high signal intensity were classified as “not diseased”. The probability of disease in the MR-CVW images was scored using the following five-point scale: 5=certainly diseased, 4=probably diseased, 3=uncertain, 2=probably not diseased, 1=certainly not diseased. A score of 4 or 5 resulted in the classification “diseased”, a score of 1-3 as “not-diseased”. On IVUS images, the high spatial resolution allows for more accurate quantification of vessel wall thickness. An ROI was classified as normal if there was no intimal thickening or intimal thickening less than 0.3 mm. A segment was classified as “diseased” on IVUS if there was visible plaque or wall thickening more than 0.3 mm [15].

Quantitative evaluation of the MR images of the RCA vessel wall was performed with the custom made software package VesselMASS. In the predefined ROIs, the inner and outer borders of the vessel wall were manually delineated. To avoid errors in thickness measurement due to reconstruction errors, only source images were used for measurements. For each ROI, minimal, maximal and mean vessel wall thickness of the right coronary vessel wall were measured.

Quantitative analysis of IVUS images was performed in QCU-CMS and consisted of offline measurement of minimal, mean and maximal vessel wall thickness in each ROI on axial source images after choosing the correct radial through the vessel.

Statistical analysis

Statistical analysis was performed with SPSS 15 for Windows (SPSS, Chicago, IL, USA). Sensitivity, specificity,

negative predictive value (NPV) and positive predictive value (PPV) were calculated based on the final diagnosis on MRI using IVUS as the standard of reference. Sensitivity and specificity for different degrees of certainty for diagnosing the presence of disease on MR-CVW were compared with the final diagnosis on IVUS, and visualised using receiver operating characteristic (ROC) curve analysis and the corresponding area under the curve (AUC). In addition, mean wall thickness as measured in matched ROIs at MR-CVW and IVUS were compared using the paired samples *t*-test. The relationship between measurements with both techniques were evaluated with linear regression analysis and visualised with Bland Altman and scatterplots. Significance was established at a *P* value of less than 0.05.

Results

Out of 75 subjects screened, 23 patients were enrolled in this study (Fig. 2), and evaluable IVUS and MR images were obtained in 17 patients. Demographic data and known risk factors of these remaining 17 patients are summarised in Table 1. No data about the CT coronary calcium score (Agatston) were available for our subjects, since not all subjects underwent a CTA of the coronary arteries. MRI and IVUS were performed in random order. Due to logistic reasons (schedule of the cardiology cathlab and limited time slots for MRI) MRI and IVUS were not performed on the same day but with a mean interval of 12 ± 10 days (range, 1-30 days). During this time interval, no changes in medication occurred except for the necessary changes in anticoagulation medication prior to elective PCI. CAG revealed significant stenoses ($\geq 50\%$) in the proximal and mid RCA of six subjects, one subject had a significant stenosis in the distal RCA, seven subjects had non-significant ($< 50\%$) stenoses in the RCA and three subjects had no angiographically visible stenoses in the RCA. Five out of the seven subjects with non-significant stenoses in the RCA underwent PCI (three patients) or FFR (two patients) of lesions in the left anterior descending or circumflex artery.

Screened (75)

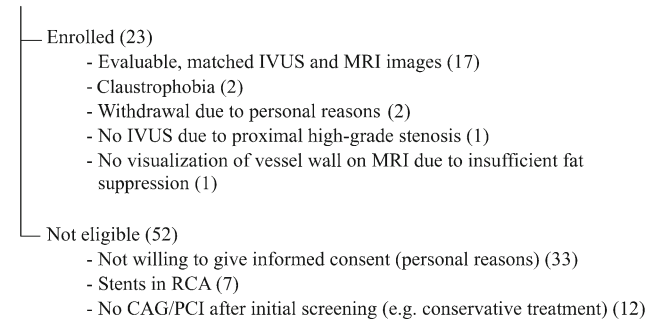


Fig. 2 Overview of screened, enrolled and excluded patients. Numbers in parentheses represent number of patients

In the included patients, the proximal, middle and often the distal part of the RCA were visualised on the MR-CVW images. As explained above, multiple short vessel wall segments in the proximal and middle RCA were used for analysis since only short ROIs could be delineated per slice. Not all of the 68 (17×4) potential ROIs could be analysed because there was a discrepancy between IVUS and MR-CVW in the number of available ROIs. Discrepancies were slightly more MR- than IVUS-related due to issues related to spatial resolution, signal-to-noise ratio and the risk of (motion) artefacts. In eight patients, less than four ROIs were available on MR-CVW due to the inability to distinguish the vessel wall from the lumen ($n=6$, all distally located in the middle RCA segments) or surrounding tissue ($n=2$). In addition, IVUS pullback distance was sometimes shorter than the visualised vessel wall on MR-CVW due to inability to insert the IVUS catheter deep enough in the RCA beyond a severe stenosis or tortuosity of the RCA ($n=3$), and in some patients the origin of the RCA was not well visualised on IVUS due to the need to insert the guiding catheter into the origin ($n=3$). In the 17 subjects for whom both MR-CVW and IVUS were available, a comparison

Table 1 Patient characteristics

Characteristics	Evaluable patients ($n=17$)
Male sex, n (%)	15 (88)
Age, years (\pm SD)	60.12 (9.06)
$\geq 50\%$ stenosis in proximal and mid RCA, n (%)	6 (35)
Weight, kg (\pm SD)	83.47 (12.89)
Systolic blood pressure, mm Hg (\pm SD)	134 (11.03)
Diastolic blood pressure, mm Hg (\pm SD)	77 (9.94)
Diabetes, n (%)	1 (5.9)
Current smoker, n (%)	4 (24)
Hypertension, n (%)	9 (59)
Cholesterol lowering medication, n (%)	16 (94)

Patient characteristics of the 17 patients with evaluable images

between IVUS and MR-CVW was eventually performed in 52 matched ROIs located in the proximal and middle RCA, consisting of both diseased and non-diseased segments. The mean length per ROI was 10.6 ± 2.6 mm (range, 6.2–18.5 mm). In Fig. 3, results are shown of a patient with stenosis of the proximal RCA.

Based on MRI, 15/52 (29%) segments were classified as normal and 37/52 (71%) as diseased. On IVUS, 17/52 ROIs (33%) were classified as normal, and 35/52 ROIs (67%) were classified as diseased. Based on IVUS, there was only one patient completely free of vessel wall thickening in all visualised segments. There was good agreement between MR-CVW and IVUS with regard to the assessment of disease. Based on qualitative assessment of presence of disease, sensitivity was 94%, specificity was 77%, NPV was 87% and PPV was 89%. The ROC curve demonstrated an AUC of 0.88 (95% CI, 0.76–0.99; Fig. 4). In all subjects with significant stenoses (defined as $\geq 50\%$) in the proximal and middle RCA as demonstrated by CAG, the lesion was also visualised with both IVUS and MRI.

There was disagreement between IVUS and MR-CVW with regard to the presence of disease in 6/52 vessel wall segments (12%). MR-CVW was false negative in two ROIs, and false positive in four ROIs. Comparison of IVUS and MR-CVW images demonstrated heavy calcification of the coronary vessel wall in the two false-negative ROIs (in the same patient), with preservation of normal lumen diameter. The four false positive ROIs that were seen (three patients) had mild intima hyperplasia at IVUS with a thickness of less than 0.3 mm in two ROIs and normal vessel wall thickness in the other two ROIs.

Results of vessel wall thickness measurements are listed in Table 2. With IVUS, a significantly lower vessel wall thickness was found when compared with MR-CVW (0.48 vs 1.24 mm, $P < 0.001$). There was large heterogeneity between the different measurements, resulting in a low R^2 value of 0.17 (Fig. 5). Bland Altman analysis demonstrated that the heterogeneity of measurements was independent of average vessel wall thickness (Fig. 5). However, there was a significant difference in vessel wall thickness between segments classified as normal versus segments classified as diseased on both MR-CVW (1.07 vs 1.32 mm, $P = 0.004$) and IVUS (0.27 vs 0.59 mm, $P < 0.001$).

Discussion

In the current study we found that MR-CVW imaging is able to accurately visualise areas of focal coronary artery vessel wall thickening compared with the established standard of reference, IVUS. Both segments with positive remodelling as well as wall thickening associated with coronary stenosis could reliably be detected with MR-CVW, although the

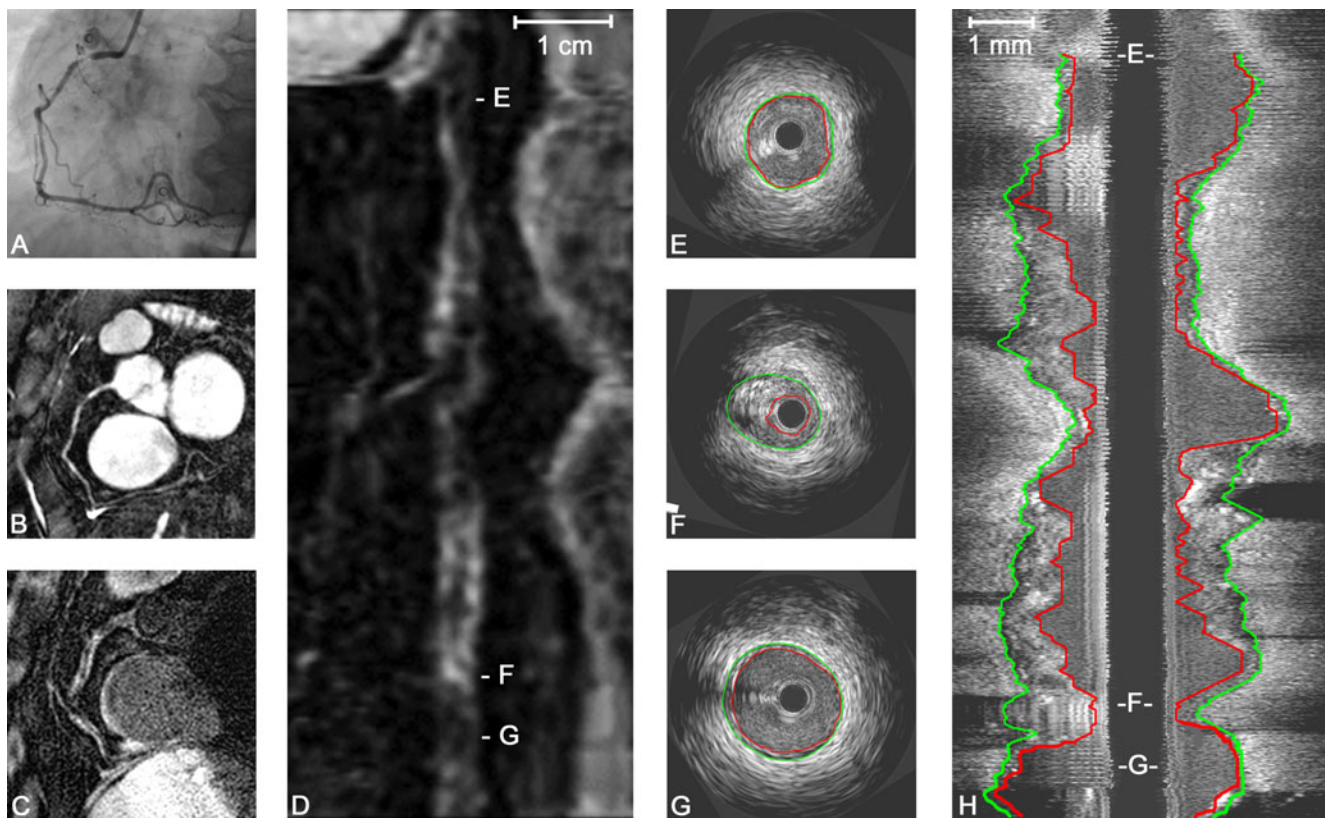


Fig. 3 A 61-year-old female patient with stable angina. X-ray angiography (a) and coronary MRA (b) demonstrate high-grade stenosis in the proximal RCA. c Corresponding MR vessel wall image demonstrate several areas with vessel wall thickening and high signal intensity. e (Distal RCA), f (diseased area) and g (proximal RCA) are cross-

sectional IVUS images and refer to the corresponding areas as shown on stretched multiplanar reformation (MPR) of the vessel wall (d: E, F, G) and the longitudinal IVUS reformat (h: E, F, G). F is the area of maximum stenosis

accuracy of absolute quantification of wall thickness is limited by the lower spatial resolution of MRI.

Although 17 subjects is a limited amount of subjects, we analysed multiple segments per subject and we believe that the segment-by-segment analysis from this pilot study gives a good impression about the possibilities and limitations of MR-CVW compared with IVUS. Due to time constraints, we limited imaging to the RCA. However, MR-CVW can also be performed in the other coronary arteries [11, 16]. Improvement of MRI technique, leading to shorter MR data acquisitions, will potentially result in better visualisation of the whole coronary tree and also in improved patient comfort, by decreasing the total length of time the patient has to stay within the MRI gantry.

Despite the capability to accurately identify location of segments of the coronary wall that harboured disease, we do acknowledge that the major limitation in accurately quantifying absolute coronary vessel wall thickness by MRI is the limited spatial resolution. We found a low correlation between absolute measurements of vessel wall thickness. Because of the lower spatial resolution of MRI compared with IVUS, we found an overestimation of wall thickness as

measured by MR-CVW. A thickness of the intima-media complex smaller than 0.3 mm is suggested as an empirical arbitrary cut-off to distinguish between atherosclerotic plaque and mild physiological intimal thickening [15]. This value of 0.3 mm at IVUS was used as the cut-off value to distinguish diseased from non-diseased coronary artery segments. The in-plane spatial resolution of the MR vessel wall sequence as used in our study was 0.78 mm. In Fig. 5, it can be seen that the mean overestimation of MR-CVW versus IVUS is approximately 0.8 mm, i.e. 1 pixel width. Objects with a size down to 1 pixel are captured with reasonable accuracy. Below that limit, full width at half maximum (FWHM) remains constant, although relative brightness of the pixel changes. Therefore, with currently used spatial resolution, small changes in wall thickness as found by IVUS cannot accurately be distinguished by measuring wall thickness on MR-CVW but are probably distinguished by changes in pixel intensity due to partial volume effects. Due to a non-isotropic voxel size, partial volume effects are mostly encountered in the slice-direction due to the slice thickness of 3 mm (reconstructed slice thickness of 1.5 mm). Vessel wall thickening was not only judged on MPR but also

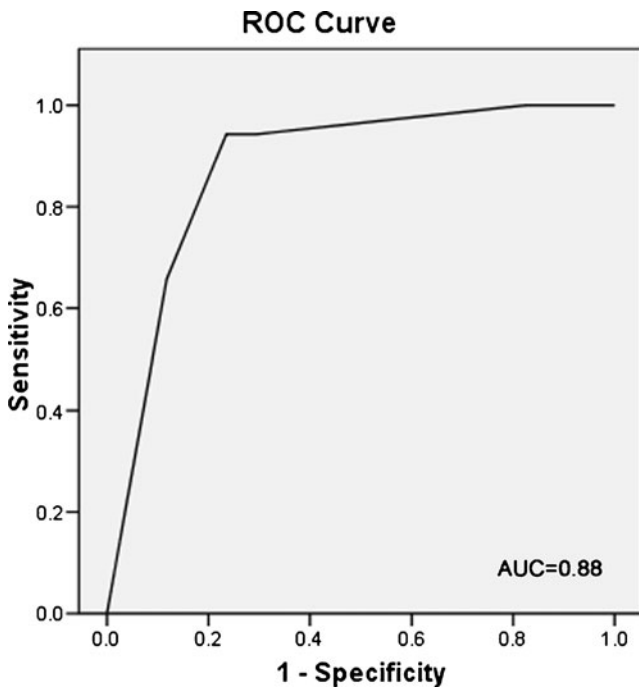


Fig. 4 Receiver operating characteristic (ROC) curve for different degrees of certainty for diagnosing the presence of disease. The area under the curve (AUC) is 0.88

on source images, and measurements were only performed on source images, this might minimise but cannot completely prevent errors. The impact of vessel curvature on the vessel wall appearance cannot completely be avoided since optimising spatial resolution in coronary vessel wall imaging is limited due to several factors (acquisition time, SNR). Further studies are needed to see whether using optimised protocols, axial imaging planes or high field MR systems would demonstrate better results.

He et al. [16] used axial MR images of the proximal coronary arteries (left main, left anterior descending, circumflex and right coronary arteries) instead of longitudinal images of the coronary vessel wall and compared these with IVUS. Although their imaging plane is obviously different than in our study, our study confirms their results regarding the capability of plaque detection with coronary vessel wall MRI. In the study by He et al., axial MR images of the proximal coronary vessel wall were used, with a spatial resolution of $1.04 \times 1.04 \times 5$ mm (which is slightly higher than in our study).

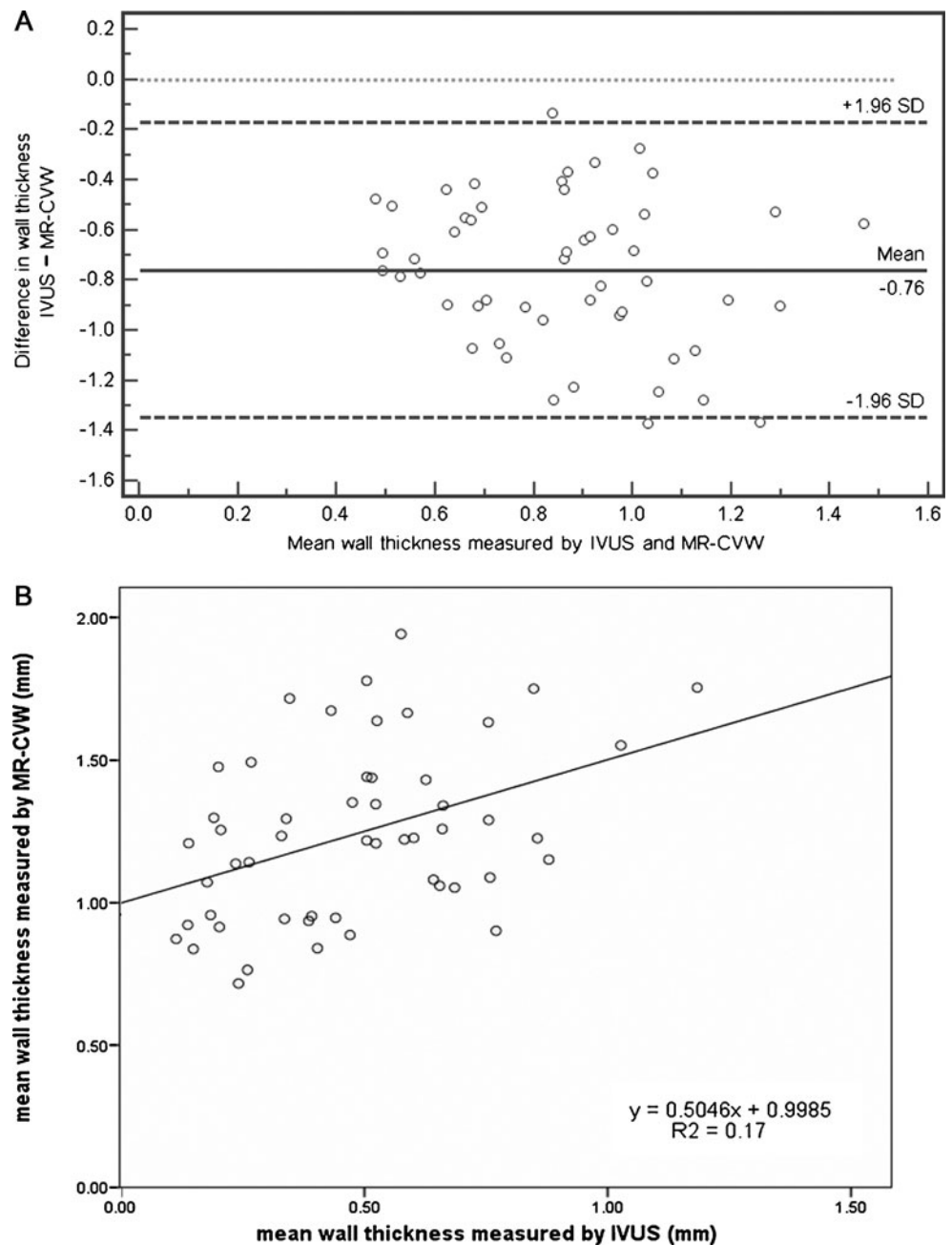
This group demonstrated good correlation between MRI and IVUS when looking at luminal cross sectional area and plaque burden as measured on MRI and IVUS in slices with plaque. As mentioned earlier, with the longitudinal imaging plane as used by our group, cross-sectional areas and plaque burden cannot reliably be assessed and therefore we limited our analysis to wall thickness measurements. However, in all slices combined (both slices with normal and diseased vessel wall), He et al. only found moderate correlation between MRI and IVUS. Although this correlation was still better than in our study, the differences in absolute wall thickness parameters between MRI and IVUS still remain. In our study we chose for larger coverage of one coronary artery—i.e. imaging the entire RCA vessel wall for analysis of the proximal and middle RCA—and, by using the longitudinal orientation, we validated the most commonly used technique for coronary vessel wall imaging, which has now been demonstrated to be capable of detecting IVUS-proven areas of thickened coronary vessel wall by using qualitative evaluation of vessel wall characteristics.

There are other potential reasons that could have caused the discrepancies which were found between MR-CVW imaging and IVUS. In this study, there was a difference in the layers of the vessel wall that were included in the measurement. On IVUS, only intima thickness was measured. At MR-CVW, different vessel wall layers cannot be distinguished and therefore measurements include intima, media and adventitia. Secondly, matching of images was challenging because of difficulties in identifying the best matching longitudinal cross-section on IVUS for the ROIs drawn on MR-CVW and also due to some distortions of the RCA on IVUS caused by the presence of an intravascular catheter and rotation of the IVUS catheter in the vessel due to vessel curvature. To minimise errors, we correlated the position of the ROIs to the origin of the RCA and the position of side branches. For future studies, plaque area or volume as measured on axial MR images instead of wall thickness measurements on longitudinal images might be a more accurate representation of plaque burden and might minimise matching errors due to slight rotation and partial volume effects in the slice encoding direction. However, this implies that the relatively fast longitudinal MR-CVW should be changed to a more time-consuming axial vessel wall sequence, which limits the area of the coronary artery

Table 2 Wall thickness measurements

	Overall (n=52)	Diseased ROIs (n=35)	Normal ROIs (n=17)	P (normal vs diseased)
Mean vessel wall thickness (mm [± SD]) in 52 matched ROIs as measured on MR-CVW and IVUS, and divided into diseased and normal ROIs				
MR-CVW (mm [± SD])	1.24 (±0.30)	1.32 (±0.30)	1.07 (±0.22)	0.004
IVUS (mm [± SD])	0.48 (±0.25)	0.59 (±0.22)	0.27 (±0.14)	<0.001
Ratio (MR/IVUS)	3.3 (±1.89)	2.6 (±1.25)	4.9 (±2.1)	<0.001
P	<0.001	<0.001	<0.001	

Fig. 5 Correlation of coronary vessel wall thickness measurements. Bland Altman plot (a) and scatterplot (b) for coronary vessel wall thickness as measured on IVUS and the MR-CVW images. There is a large heterogeneity of wall thickness measurements when IVUS is compared with MR-CVW, resulting in a low correlation coefficient ($R^2=0.17$)



that can be covered in the same imaging time. For instance, axial imaging was performed in a large cohort in the Multi-Ethnic Study of Atherosclerosis (MESA) [17], although in that study only the proximal portions of the main coronary arteries were analysed due to time constraints, and a maximum of seven slices were acquired per patient.

Thirdly, we used a double inversion recovery technique to suppress blood in the RCA. This technique is flow dependent, and in the present study only the blood in the proximal and middle parts could reliably be suppressed on MR-CVW. Inadequate suppression of (slow-flowing) blood at the lumen-vessel wall interface might be the cause of overestimation of wall thickness in the four false-positive vessel segments. As

expected, this phenomenon occurred mostly in the non-proximal parts of the RCA (3/4 cases).

Another factor that might influence wall thickness measurements is calcification of the vessel wall, which can lead to underestimation of wall thickness or even the inability to visualise the vessel wall, since calcification has a very low signal intensity on MR sequences [18, 19]. In our study we encountered two false-negative ROIs on MR-CVW, corresponding IVUS images demonstrated calcification of the vessel wall with preservation of the lumen. However, in other calcified ROIs as seen with IVUS, there was agreement between IVUS and MR-CVW. Thus, a pitfall for MR-CVW would be the presence of calcified plaque, especially

in an area with positive remodelling. However, heavy calcification also causes artefacts in IVUS and in computed tomography (CT), thereby decreasing the ability for analysis of plaques and, especially in CT, the degree of stenosis [20, 21].

Finally, there were some differences in acquisition between IVUS and MRI: First, image acquisition in MRI is done in mid-diastole, whereas in IVUS images are acquired during the entire cardiac cycle. Nakatani et al. [22] demonstrated only minimal variations in luminal area during the cardiac cycle, and it is likely that variation in luminal area and diameter exceed variation in absolute vessel wall thickness over the cardiac cycle. Therefore, we expect that differences in vessel wall thickness during the cardiac cycle are averaged and so small that these differences do not influence the results significantly, especially considering the spatial resolution used. Another difference in acquisition was the use of nitroglycerine as a vasodilating agent in the IVUS procedure but not in MRI. Nitroglycerine has a major effect on the lumen diameter of coronary arteries, causing significant dilatation [23]. However, nitroglycerine-induced dilatation is reported to be impaired in areas with atherosclerosis [22, 24], as was the case in many of our studied ROIs. The effect of nitroglycerine on absolute coronary vessel wall thickness measurements is not precisely known, but again we do expect that these small differences are beyond the limit of detection with MRI. However, we do plan to use nitroglycerine in future studies to minimise possible differences in measurements.

In conclusion, this study demonstrated the ability of MR-CVW to accurately detect the presence and location of coronary vessel wall thickening in the RCA when compared with IVUS, the standard of reference for coronary vessel wall imaging. However, as expected due to differences in spatial resolution, MR-CVW systematically overestimates absolute coronary vessel wall thickness and is therefore not recommended for absolute vessel wall thickness measurements when a longitudinal acquisition orientation is used.

Acknowledgements The authors would like to thank Boston Scientific Benelux B.V. for their training in and assistance with acquiring the IVUS-images. Furthermore, we would like to thank all interventional cardiologists working in the Maastricht University Medical Centre, for their assistance with IVUS procedures.

This study was supported by BayerSchering Pharma. The sponsor had no influence on study design, data collection or analysis of the data.

Trial registration:www.clinicaltrials.gov ID: NCT00984776

References

- Glagov S, Weisenberg E, Zarins CK, Stankunavicius R, Kolettis GJ (1987) Compensatory enlargement of human atherosclerotic coronary arteries. *N Engl J Med* 316:1371–1375
- Libby P (2002) Inflammation in atherosclerosis. *Nature* 420:868–874
- Schoenhagen P, Ziada KM, Kapadia SR, Crowe TD, Nissen SE, Tuzcu EM (2000) Extent and direction of arterial remodeling in stable versus unstable coronary syndromes: an intravascular ultrasound study. *Circulation* 101:598–603
- Losordo DW, Rosenfield K, Kaufman J, Pieczek A, Isner JM (1994) Focal compensatory enlargement of human arteries in response to progressive atherosclerosis. In vivo documentation using intravascular ultrasound. *Circulation* 89:2570–2577
- Fayad ZA, Nahar T, Fallon JT et al (2000) In vivo magnetic resonance evaluation of atherosclerotic plaques in the human thoracic aorta: a comparison with transesophageal echocardiography. *Circulation* 101:2503–2509
- Yuan C, Beach KW, Smith LH Jr, Hatsukami TS (1998) Measurement of atherosclerotic carotid plaque size in vivo using high resolution magnetic resonance imaging. *Circulation* 98:2666–2671
- Corti R, Fuster V, Fayad ZA et al (2002) Lipid lowering by simvastatin induces regression of human atherosclerotic lesions: two years' follow-up by high-resolution noninvasive magnetic resonance imaging. *Circulation* 106:2884–2887
- Adams GJ, Greene J, Vick GW 3rd et al (2004) Tracking regression and progression of atherosclerosis in human carotid arteries using high-resolution magnetic resonance imaging. *Magn Reson Imaging* 22:1249–1258
- Botnar RM, Stuber M, Kissinger KV, Kim WY, Spuentrup E, Manning WJ (2000) Noninvasive coronary vessel wall and plaque imaging with magnetic resonance imaging. *Circulation* 102:2582–2587
- Kim WY, Stuber M, Bornert P, Kissinger KV, Manning WJ, Botnar RM (2002) Three-dimensional black-blood cardiac magnetic resonance coronary vessel wall imaging detects positive arterial remodeling in patients with nonsignificant coronary artery disease. *Circulation* 106:296–299
- Botnar RM, Kim WY, Bornert P, Stuber M, Spuentrup E, Manning WJ (2001) 3D coronary vessel wall imaging utilizing a local inversion technique with spiral image acquisition. *Magn Reson Med* 46:848–854
- Austen WG, Edwards JE, Frye RL et al (1975) A reporting system on patients evaluated for coronary artery disease. Report of the Ad Hoc Committee for Grading of Coronary Artery Disease, Council on Cardiovascular Surgery, American Heart Association. *Circulation* 51:5–40
- Dijkstra J, Koning G, Reiber JH (1999) Quantitative measurements in IVUS images. *Int J Card Imaging* 15:513–522
- Adame IM, van der Geest RJ, Wasserman BA, Mohamed MA, Reiber JH, Lelieveldt BP (2004) Automatic segmentation and plaque characterization in atherosclerotic carotid artery MR images. *MAGMA* 16:227–234
- Di Mario C, Gorge G, Peters R et al (1998) Clinical application and image interpretation in intracoronary ultrasound. Study Group on Intracoronary Imaging of the Working Group of Coronary Circulation and of the Subgroup on Intravascular Ultrasound of the Working Group of Echocardiography of the European Society of Cardiology. *Eur Heart J* 19:207–229
- He Y, Zhang Z, Dai Q et al (2012) Accuracy of MRI to identify the coronary artery plaque: a comparative study with intravascular ultrasound. *J Magn Reson Imaging* 35:72–78
- Miao C, Chen S, Macedo R et al (2009) Positive remodeling of the coronary arteries detected by magnetic resonance imaging in an asymptomatic population: MESA (Multi-Ethnic Study of Atherosclerosis). *J Am Coll Cardiol* 53:1708–1715
- Toussaint JF, LaMuraglia GM, Southern JF, Fuster V, Kantor HL (1996) Magnetic resonance images lipid, fibrous, calcified, hemorrhagic, and thrombotic components of human atherosclerosis in vivo. *Circulation* 94:932–938
- Leiner T, Gerretsen S, Botnar R et al (2005) Magnetic resonance imaging of atherosclerosis. *Eur Radiol* 15:1087–1099

20. Stolzmann P, Scheffel H, Leschka S et al (2008) Influence of calcifications on diagnostic accuracy of coronary CT angiography using prospective ECG triggering. *AJR Am J Roentgenol* 191:1684–1689
21. Ong TK, Chin SP, Liew CK et al (2006) Accuracy of 64-row multidetector computed tomography in detecting coronary artery disease in 134 symptomatic patients: influence of calcification. *Am Heart J* 151:1323.e1–1323.e6
22. Nakatani S, Yamagishi M, Tamai J et al (1995) Assessment of coronary artery distensibility by intravascular ultrasound. Application of simultaneous measurements of luminal area and pressure. *Circulation* 91:2904–2910
23. Decramer I, Vanhoenacker PK, Sarno G et al (2008) Effects of sublingual nitroglycerin on coronary lumen diameter and number of visualized septal branches on 64-MDCT angiography. *AJR Am J Roentgenol* 190:219–225
24. Yamagishi M, Nissen SE, Booth DC et al (1995) Coronary reactivity to nitroglycerin: intravascular ultrasound evidence for the importance of plaque distribution. *J Am Coll Cardiol* 25:224–230